

Long-Term Electrochemical Criteria for Crevice Corrosion in Concentrated Chloride Solutions

T. Ahn,¹ X. He,² H. Jung² and P. Shukla²

¹U.S. Nuclear Regulatory Commission, Washington, DC

²Center for Nuclear Waste Regulatory Analyses, San Antonio, TX

Abstract

Crevice corrosion is the predominant mode of localized corrosion of Alloy 22 in concentrated chloride solutions of near-boiling temperatures and high to moderate humidity. A literature review was performed to assess whether the repassivation potential or the breakdown potential can be applied in forecasting the initiation of crevice corrosion of Alloy 22 over very long periods of time (e.g., hundreds of thousands of years). Specifically, this review presents (i) environments and crevice corrosion criteria, (ii) data and models for Alloy 22 crevice corrosion, and (iii) induction times for crevice corrosion. With forced applied current between the anode and the cathode of a crevice cell, crevice corrosion may be initiated/sustained at the corrosion potential above the repassivation potential. At the free open-circuit corrosion potential, however, crevice corrosion may not be initiated/sustained until the corrosion potential reaches the breakdown potential. Characteristics of crevice corrosion propagation are also discussed. Models for the induction time for localized corrosion are evaluated to assess whether laboratory tests can be used to forecast the potential for crevice corrosion development over very long periods of time. Data on the initiation for crevice corrosion measured in laboratory time periods appear to scale appropriately for extrapolation to very long periods of time, such as hundreds of thousands of years.

1. Introduction

Crevice corrosion is the predominant mode of localized corrosion of Alloy 22 in concentrated chloride solutions of near-boiling temperatures and high to moderate humidity. The objective of this work is to review relevant literature data on the electrochemical criteria for the initiation of crevice corrosion. Two electrochemical criteria, breakdown potential and repassivation potential, have been considered in the literature. When the corrosion potential reaches above the breakdown potential, the literature suggests that protective passive oxide film formed on the metal surface is destabilized, causing localized corrosion or transpassive dissolution. When the corrosion potential is lowered below the repassivation potential, the destabilized passive oxide film becomes restabilized. The breakdown potential is higher than or equal to the repassivation potential. This work assesses the applicability of the breakdown potential and the repassivation potential for assessing crevice corrosion. It also addresses the characteristics of crevice corrosion propagation. Additionally, models for the induction

time to initiate localized corrosion are evaluated to assess whether laboratory tests represent the very long-term performance in crevice corrosion. For this purpose, this review presents specifically (i) environments and crevice corrosion criteria, (ii) data and models for Alloy 22 crevice corrosion, and (iii) induction times for crevice corrosion.

2. Data and Models for Alloy 22 Crevice Corrosion

Crevice Corrosion under Potentiostatic Conditions

Szklarska-Smialowska presented a general concept of the potentiostatic electrochemical criteria for localized corrosion [Szklarska-Smialowska, 1986]. Figure 1 shows different stages of localized corrosion Fe-1Cr single crystal in 0.4N NaCl + 0.7N Na₂SO₄ as an example case. The number of pits are plotted for various applied potentials.

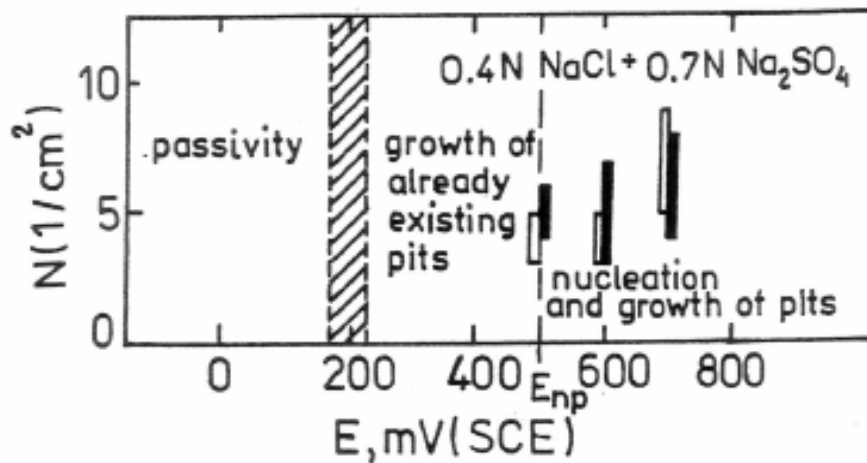


Figure 1. Example of Different Stages of Localized Corrosion Number of pits (stationary value) vs. potential for (110) and (111) planes of Fe-1Cr single crystals. E_{np} is potential of pit nucleation and marked by rectangles [Szklarska-Smialowsak, NACE, 1986].

Figure 1 suggests that localized corrosion as pitting corrosion and crevice corrosion could occur in various stages depending on the applied potential.

- (i) $E_{break} < E_{corr}$: localized corrosion initiation
- (ii) $E_{repass} < E_{corr} < E_{break}$: propagation of existing localized corrosion
- (iii) $E_{corr} < E_{repass}$: no localized corrosion initiation

E_{corr} , E_{break} , and E_{repass} are corrosion potential, breakdown potential, and repassivation potential, respectively. ASM Handbook also presents a similar assessment. For metals that have good resistance to pitting, the second stage, (ii), will not initiate/propagate pitting corrosion [ASM International, 1987]

For nickel-based alloys, Alloy 825, 625 and 22, Dunn, et al., measured the initiation times for the crevice corrosion in 5.5 M NaCl solution at 100 °C as shown in Figure 2 [Dunn, et al., 2005]. The initiation times were measured under potentiostatic conditions. The initiation time was increased as the applied potential was lowered toward the repassivation potential. This indicates that the repassivation potential is a long-term threshold potential for the initiation of crevice corrosion. Figure 2 also presents breakdown potentials under cyclic potentiodynamic polarization (CPP) conditions for comparison with potentiostatic conditions. E_{rcrev} is the repassivation potential for crevice corrosion and E_{applied} is the applied potential.

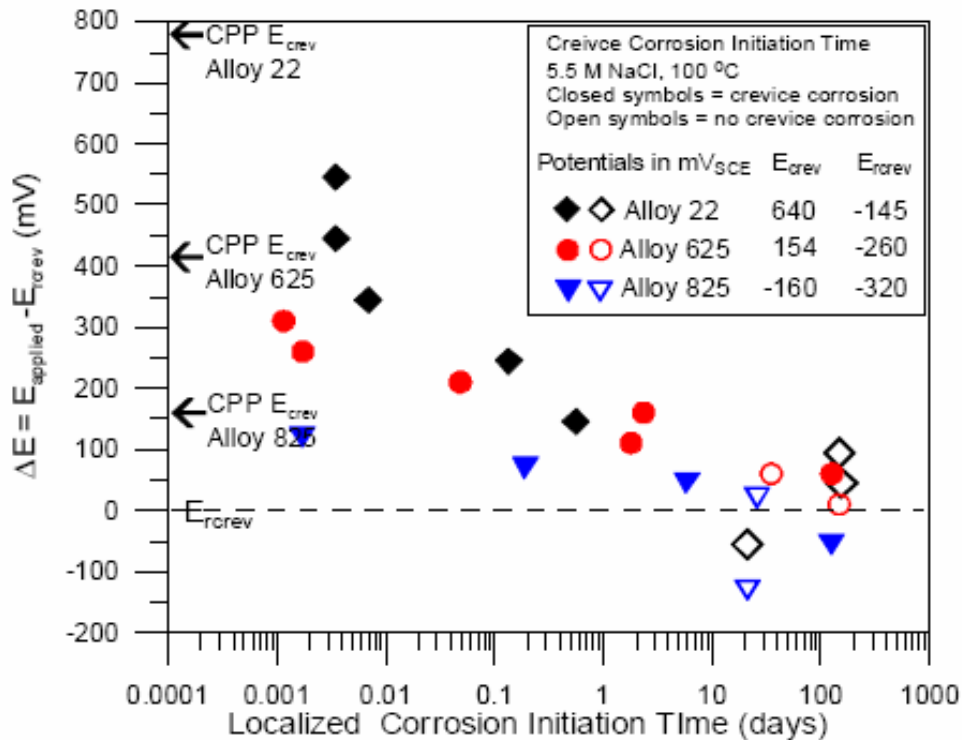


Figure 2. Initiation Time for Crevice Corrosion As a Function of Applied Potential for Alloys 825, 625, and 22 in 5.5 M NaCl at 100 °C [212 °F]. Initiation Times Measured Under Potentiostatic Conditions.

Note: CPP—Cyclic potentiodynamic polarization [Dunn, et al., 2005]

Crevice Corrosion under Free Open-circuit Corrosion Conditions

He and Dunn monitored current densities and potentials using the single crevice assembly for an Alloy 22 cylindrical specimen galvanically coupled to a large Alloy 22 plate in 5M NaCl solution with addition of 2×10^{-4} M CuCl_2 at 95 °C [203 °F] [He and Dunn, 2005]. CuCl_2 was added to simulate the free open-circuit corrosion conditions for the initiation

of crevice corrosion by increasing the corrosion potential near the breakdown potential. The initiation conditions were obtained without applying continuously forced current as used in the potentiostatic method. Figure 3 shows schematics of the electrochemical test cell with single crevice assembly to study the crevice corrosion. The Alloy 22 cylindrical specimen was galvanically coupled to Alloy 22 through a zero resistance ammeter and a volt meter to measure the potential of the galvanic couple against the reference saturated calomel electrode (SCE).

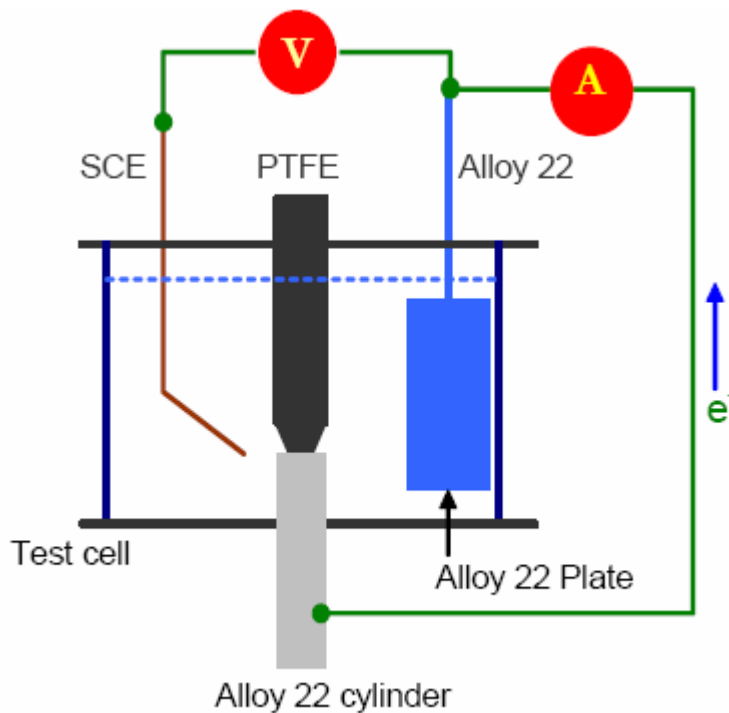


Figure 3. Schematics of the Electrochemical Test Cell with Single Crevice Assembly to Study the Crevice Corrosion Propagation in Alloy 22
(Note: PTFE–Polytetrafluoroethylene; SCE–Saturated Calomel Electrode)
[He and Dunn, 2005]

Figure 4 shows the measured current density and the potential. By adding CuCl_2 , the current density and potential increased to $1 \times 10^{-4} \text{ A/cm}^2$ [$1.6 \times 10^{-5} \text{ A/in}^2$] and $429 \text{ mV}_{\text{SCE}}$, respectively. Potentials were compared with Figure 2 where the test conditions were nearly identical except adding the oxidizer. The initial potential appears to be in the range of the breakdown potential, because the current density represents the passivity breakdown [Rodriguez, et al., 2007]. This potential is also close to the breakdown

potential, $640 \text{ mV}_{\text{SCE}}$, well above the repassivation potential, $-145 \text{ mV}_{\text{SCE}}$, from Figure 2. Currently, the breakdown potential is not well defined. The crevice corrosion was initiated by adding the oxidizer. The potential decreased as the crevice chemistry formed near the repassivation potential before the repassivation occurred. Upon the repassivation, the potential increased near to $400 \text{ mV}_{\text{SCE}}$. The crevice corrosion was not sustained at the potential well above the repassivation potential.

It appears that the crevice corrosion will not be sustained with time under free open-circuit corrosion conditions. With time the outer cathode will have thicker and crystallographically more perfect passive film, decreasing electrochemical reaction rates. The active pits formed inside the crevice and the outside cathode will be connected more weakly as the distance becomes furthered as pits grow. The crevice gaps will be widened as corrosion progresses. As a consequence of these, the electric throwing power between the cathode and the anode becomes weaker in the formed crevice corrosion cell. In a later time the figure shows that the current density drops rapidly and the potential goes up accordingly, resulting in sustaining the repassivation of the crevice corrosion.

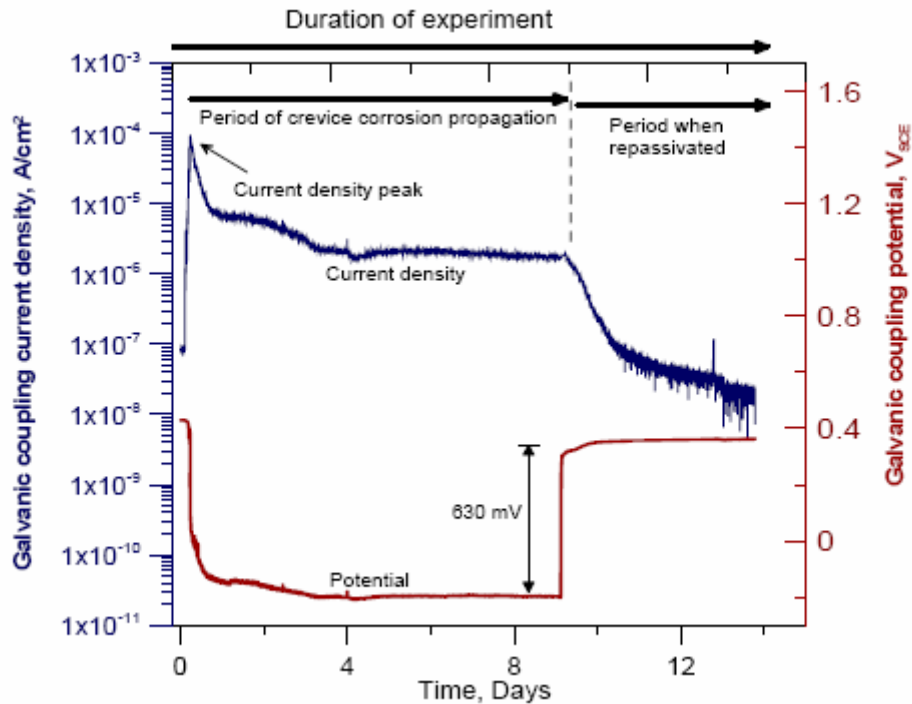


Figure 4. Measured Current Density and Potential Using the Single Crevice Assembly for an Alloy 22 Cylindrical Specimen Galvanically Coupled to a Large Alloy 22 Plate in 5 M NaCl Solution with the Addition of $2 \times 10^{-4} \text{ M CuCl}_2$ at $95 \text{ }^\circ\text{C}$ [$203 \text{ }^\circ\text{F}$], mV_{SCE} [He and Dunn, 2005]

After the test, the damage of Alloy 22 was characterized. Initially, the total crevice area was corroded. Gradually, corrosion propagation was localized to pits inside the crevice area. The pit density decreased gradually. In the end, only a few pits of the size 10 – 100

micrometer $[(4 - 39) \times 10^{-3} \text{ inch}]$ were active, and eventually the total crevice area was completely repassivated.

Dunn, et al. [2005] conducted similar open-circuit crevice corrosion tests for Alloy 22 in 5M NaCl. Tests were performed by galvanically coupling an Alloy 22 crevice specimen to an Alloy 22 plate. With an addition of CuCl_2 at 100°C [212°F], the initial potential of the couple was $260 \text{ mV}_{\text{SCE}}$, and the current density was in the passive state. With an increased concentration of CuCl_2 at 100°C [212°F], the initial potential of the couple was $410 \text{ mV}_{\text{SCE}}$, and the crevice corrosion was initiated.

In the immersion tests of Alloy 22 in $18 \text{ M CaCl}_2 + 0.9 \text{ M Ca(NO}_3)_2$ at 155°C [311°F] for 588 days, E_{corr} showed oscillations of up to 600 mV (Ag/AgCl reference electrode) during the entire immersion period [Rodriguez, et al., 2007]. At this ratio of chlorides to nitrates, crevice corrosion was expected to occur. These oscillations were due to pitting corrosion development outside the crevice. Because pitting corrosion was active outside the crevice, the concentration cell for crevice corrosion may not have formed. From the cyclic potentiodynamic polarization test after the immersion test, the breakdown potentials were 547 to 690 mV and the repassivation potentials were 31 to 35 mV , depending on the defined current densities for the breakdown potential and the repassivation potential. Figures 7 and 8 show the polarization curve and the open-circuit potential oscillation. The discussed sample number was KE0272. When the corrosion potential reaches the breakdown potential, pitting occurs. Figure 5 shows that KE0272 has the breakdown potential near 520 mV (Ag/AgCl). As the bare metal surface is exposed in the pits, the corrosion potential drops until the pits become repassivated at a potential above the repassivation potential. The corrosion potential will go up again continuously to the breakdown potential. This potential shift will be repeated, resulting in the oscillation of the corrosion potential. In other four cases (including solution heat treatments) of $18 \text{ M CaCl}_2 + 0.9 \text{ M Ca(NO}_3)_2$ (KE0242 to KE0245), pitting was observed in only one case. This suggests that pitting corrosion occurs only when the corrosion potential reaches the breakdown potential. The averaged corrosion potentials of KE0272 and KE0242 to KE0245 increased with time. As observed in the potentiostatic condition of the initiation of localized corrosion (Figure 2), the long initiation time for pitting or crevice corrosion were not noticed in this open-circuit tests.

For the tests done in $\text{CaCl}_2 + 9 \text{ M Ca(NO}_3)_2$ solution with ten times more nitrates, no pitting or crevice corrosion was observed for all samples, as expected at the low ratio of chlorides to nitrates. The corrosion potentials were less than the repassivation potential and the breakdown potential. The averaged corrosion potential decreased with time. The corrosion potential was oscillated in this solution too, but the frequency or the amplitude of the oscillation was less than the case of 0.9 M nitrates. The cause for the oscillation was unknown.

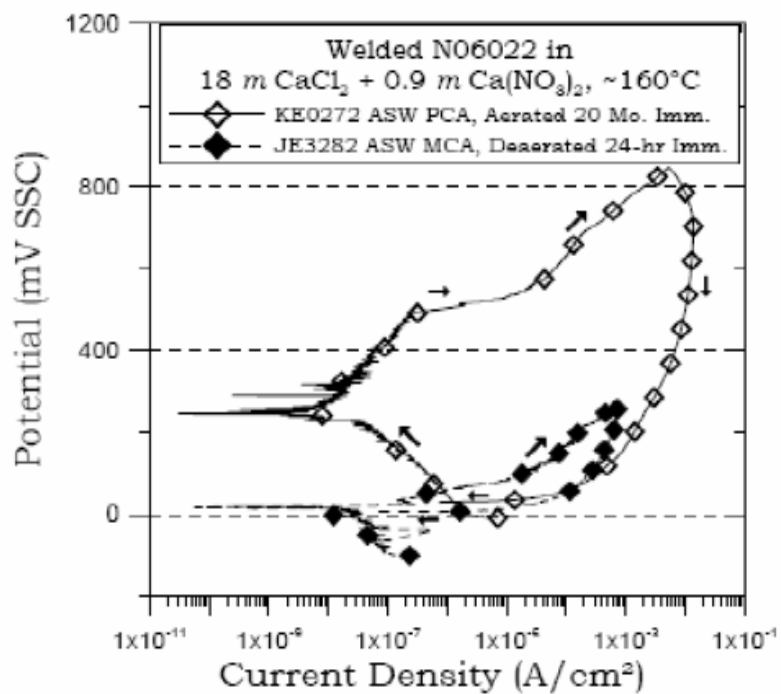


Figure 5. Cyclic Potentiodynamic Polarization for Alloy 22 in 18 M CaCl₂ + 0.9 mCa(NO₃)₂, [NO₃⁻]/[Cl⁻] = 0.05 at ~ 160 °C [320 °F] Comparing Short and Long Term Immersion. Short Term Data Is at 160 °C [320 °F] , Long Term at 155 °C [311 °F] [Rodriguez, et al., NACE, 2007]

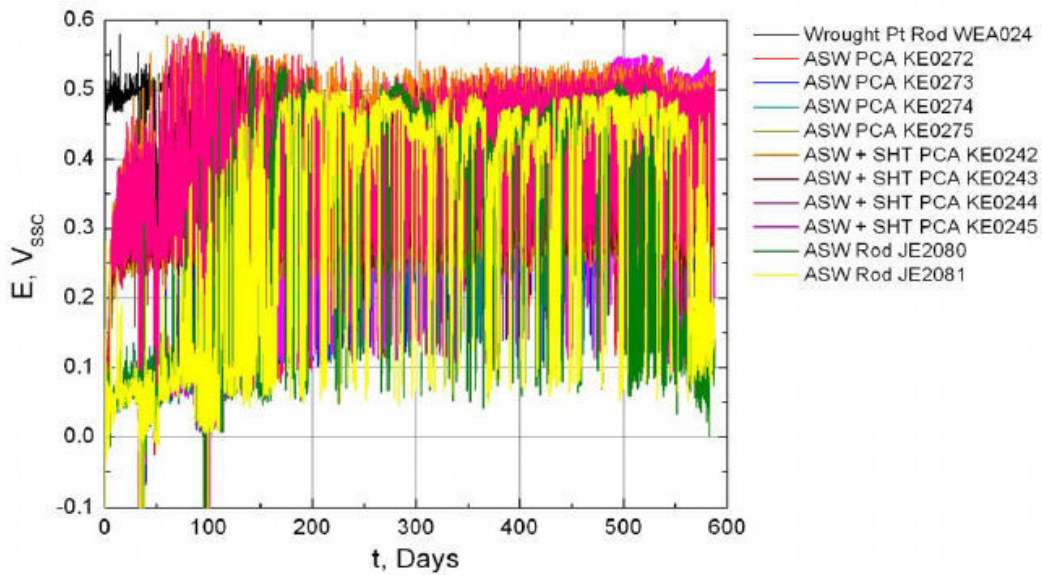


Figure 6. Corrosion Potential as a Function of Immersion Days for Alloy 22 Specimens in 18 M $\text{CaCl}_2 + 0.9 \text{ M Ca(NO}_3)_2$ [Rodriguez, et al., NACE, 2007]

In more severe environments, galvanically coupled open-circuit tests of creviced Alloy 22 [He and Dunn, 2005] were performed in 4 M MgCl_2 solution without adding oxidizers or inhibitors at 95 °C [203 °F] [He and Dunn, 2007]. Crevice corrosion was initiated under open circuit conditions. The open circuit potential decreased after crevice corrosion initiation to values close to the crevice corrosion repassivation potential. The breakdown potential was close to the crevice corrosion repassivation potential. Most crevice sites were corroded. However, the penetration depth was limited, and the deepest penetration was confined to a small area.

Figure 7 below summarized the behavior of the breakdown potential and the repassivation potential of an analog nickel-based Alloy 825 at 95 °C [203 °F] at various chloride concentrations [Sridhar, et al., 1995]. Pitting potential, E_p , is equivalent to E_{break} , and E_{rp} is E_{repass} . At high concentrations of chloride above 1 M, two potentials merge.

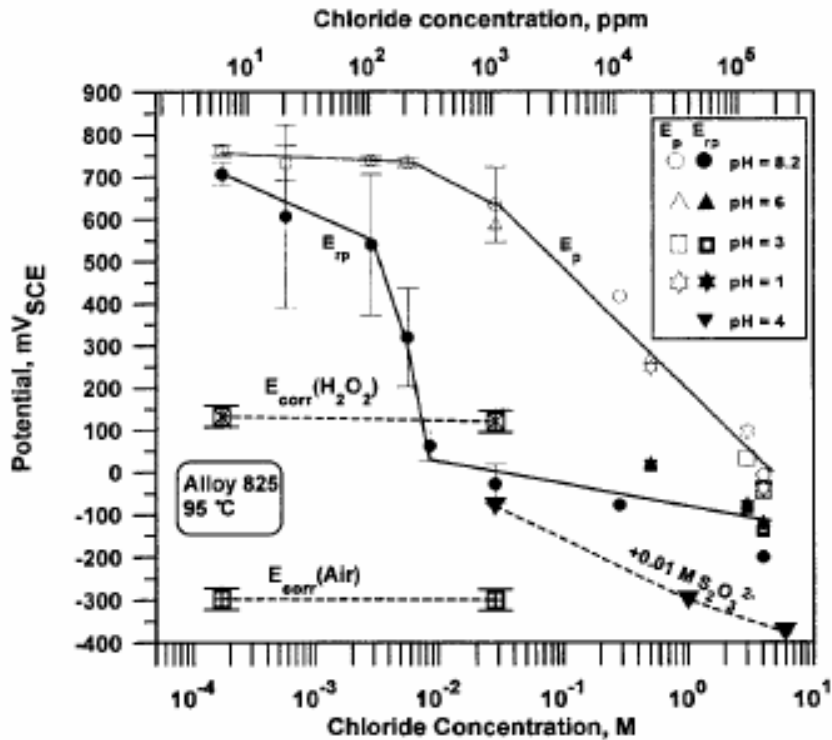


Figure 7. Effect of chloride, thiosulfate, and pH on E_p and E_{rp} for Alloy 825 at 95 °C [203 °F [Sridhar, et al., 1995]. Pitting potential (E_p) is equivalent to E_{break} and E_{rp} is E_{repass}

Models for Capacity and Modification of Cathode in Crevice Corrosion under Free Open-Circuit Corrosion Conditions

Models for cathode modification were presented to partly support this hypothesis of the repassivation of crevice corrosion under open-circuit corrosion conditions. Shukla, et al., modeled cathode capacity assuming active crevice corrosion at the anodic site [Shukla, et al., 2008]. The thickness of thin film groundwater on the cathode surface was varied. The cathode capacity was defined as the amount of excess cathode current that will balance the metal dissolution current. Figures 8 shows examples of the calculated results. The limited quantity of brine will control the rate of oxygen reduction. The cathode capacity decreases as E_{corr} decreases toward E_{rp} . The thickening or more perfection of passive film in the outer area of crevice will decrease electrochemical reaction kinetics (e.g., exchange current density).

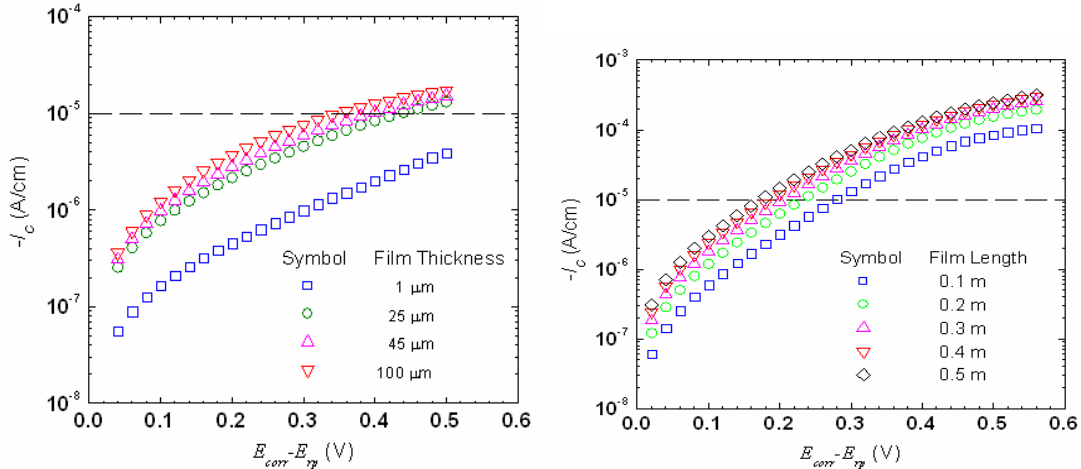


Figure 8. Capacity and Modification of Cathode in Crevice Corrosion at Open-Circuit Cathode Capacity: the amount of excess cathodic current that will balance metal dissolution is presented varying the quantity of brine (film thickness or film length) and $(E_{\text{corr}} - E_{\text{tp}})$ [Shukla, et al., 2008]

Perspectives on Crevice Corrosion Initiation Criteria

To initiate/sustain crevice corrosion in concentrated chloride solutions, the corrosion potential needs to reach the breakdown potential. For tests in 5 M NaCl solution with the addition of 2×10^{-4} M CuCl_2 at 95 °C [203 °F] [He and Dunn, 2005], the initially formed crevice corrosion at 429 mV_{SCE} was repassivated at the potential well above the repassivation potential. This could happen by the cathode surface modification, the increase of the distance between the anode and the cathode, and the increase of the crevice gap, resulting in the decrease of electric throwing power between the anode and the cathode. In the same earlier tests at the initial potential, 260 mV_{SCE}, by varying CuCl_2 concentration, the current density was in the passive state [Dunn, et al., 2005]. Similarly, in 8 M $\text{CaCl}_2 + 0.9$ M $\text{Ca}(\text{NO}_3)_2$ [Rodriguez, et al., NACE, 2007], pitting corrosion was dominant outside the crevice, and was observed only when the corrosion potential reached the breakdown potential. For both cases of two different solution tests, the corrosion potentials in repassivation were well above the repassivation potential. Models suggest that cathode capacity decreases as the corrosion potential decreases (at above the repassivation potential). In more severe environments of 4 M MgCl_2 solution without adding oxidizers or inhibitors at 95 °C [203 °F] [He and Dunn, 2007], the breakdown potential and the repassivation potential were close to each other. Therefore, the corrosion penetration depth in the crevice was limited, and the deepest penetration was confined to a small area. On the other hand under potentiostatic conditions, the electric throwing power is continuously supplied by force. Therefore, it appears that crevice corrosion could occur and be sustained at potentials as low as the repassivation potential.

To understand the criteria for crevice (or localized) corrosion criteria, it is necessary to determine values of these potentials including monitoring the corrosion potential continuously with time. Although in the tests by Rodriguez, et al. [2007], these values were partially measured, it is unclear whether the repassivation potential and the breakdown potential were measured based on the averaged current density with time or whether they truly represented the microstructural characteristics of localized attack. More data may be necessary to define these potentials and to generalize the relationship of the localized corrosion and these potentials.

3. Induction Times for Crevice Corrosion

For the long-term prediction of localized corrosion, it is necessary to understand whether the measurement of the critical potential such as the breakdown potential or the repassivation potential indeed represents the very long-term behavior. To test this hypothesis, models developed for the induction times for pitting corrosion by Lin, et al. [1981] and Urquidi-Macdonal and Macdonald [1987] are evaluated. The models predict the induction times for pitting corrosion of passive iron or carbon steel in borate buffer solution by varying chloride concentrations and pH at 25 °C [77 °F]. The equation and the figure 9 below present the results.

$$t_{ind} = \frac{\zeta}{\epsilon} \left[\exp\left\{ \frac{\gamma F \alpha \Delta V}{2 R T} \right\} - 1 \right]^{-1}$$

ΔV : applied potential minus the critical potential
(i.e., pitting potential or breakdown potential)

γ : charge on a cation

F : Faraday constant

R : gas constant

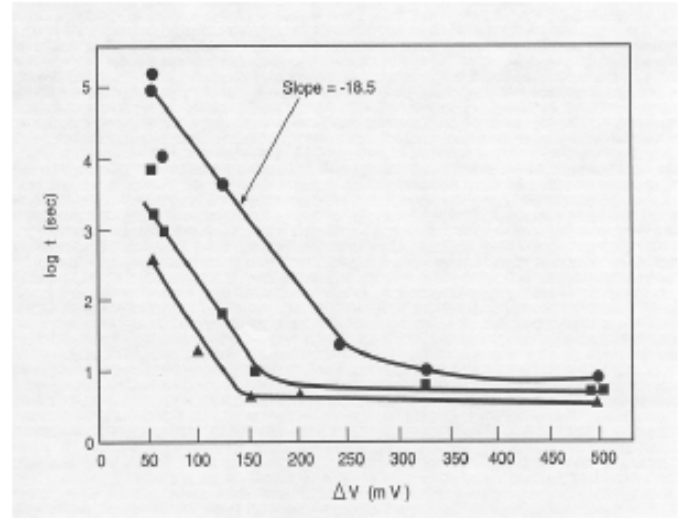
T : temperature

ζ : transient aqueous diffusion time

α : a constant relating the potential drop at the film/solution interface and applied potential, and

ϵ : a function of chloride activity, critical potential, diffusivity of cation vacancy, and a critical amount of metal holes.

(Lin et al., 1981; Urquidi-Macdonald and Macdonald, 1987)



Induction Time vs. ΔV
Data for Pitting of Passive Iron in Borate Buffer Solution at 25 °C (77 °F)
Triangle: pH 7.3 0.1M NaCl, Rectangle: pH 7.3 0.01M NaCl, Circle: pH 8.3 0.01M NaCl
(Lin et al., 1981)

Figure 9. Models and Data for Induction Times for Pitting Corrosion

When the applied potential (or corrosion potential) reaches the theoretical critical potential, the induction time becomes infinite in the equation of Figure 9. If the applied potential (or corrosion potential) exceeds the critical potential as low as 50 mV, the induction time becomes short enough to be determined in the laboratory tests as shown in Figure 9. This 50 mV is within the uncertainty limit in the very long-term corrosion potential. In the model, the distribution of the critical potential was also formulated. Increasing the distributed induction time from the averaged induction time of 100 seconds to ~ one year, the frequency of pitting decreased to be negligible. In the experiments, similar behavior of the decreased frequency was observed. The pit density inside the crevice decreased gradually with time, as discussed in the previous section. This discussion above is more about the breakdown potential. For the repassivation potential, the induction times for the crevice (or pitting) corrosion under potentiostatic conditions will behave similarly [Dunn, et al., 1996]. There will be a sharp dependence of the induction time on the corrosion (or applied) potential near the critical potential. The repassivation process involves solid-state nucleation process (e.g., oxide reformation, Okada, 1984) that has typically such a sharp dependence of the induction time on the driving force for nucleation (e.g., the applied potential).

The equations for induction time and its distribution were based on the point defect models of passive film of carbon steel and passive iron. The excess amount of cation vacancies form voids at the metal-oxide interface in the p-type passive oxide film of carbon steel in 0.8 M NaCl + 0.1 M CuCl₂ solutions at 250 °C [482 °F] [Macdonald, 1992]. The point defect model was partly adopted for the Alloy 22 model too to explain the transpassive dissolution of p-type passive film in saturated NaCl solutions at 80 °C [176 °F] [Macdonald, et al., 2004]. Therefore, the formula described above for passive iron and carbon steel may be applicable to Alloy 22.

Another type of induction time also needs to be considered in the long-term prediction of crevice corrosion. There could be prolonged times necessary to reach the critical chemistry inside the crevice from slow mass transport of dissolve species in and out of the crevice. Mass transport models were developed to reach times for constant potentials and pH arriving inside the crevice as a function of the position from the crevice mouth and laboratory test times [Combrade, 2001; Shinohara, et al., 1997; Walton, et al., 1996]. All models show short induction times within the laboratory measurement times.

Theoretical models were evaluated for electrochemical induction times for pitting corrosion (possibly inside the crevice) and for mass transport kinetics for crevice corrosion. In both cases, the long-term steady states can be reached in the laboratory time scale, because the induction times are short within the uncertainties of the measurements.

4. Summary

1. The electrochemical criteria for the initiation of crevice corrosion in concentrated chloride solutions were reviewed. An assessment was made about the potential applicability of the laboratory criteria to Alloy 22 corrosion in the very long period of time.
2. With forced applied current between the anode and the cathode of a crevice cell, crevice corrosion may be initiated at the corrosion potential above the repassivation potential.
3. At the free open-circuit corrosion potential, however, crevice corrosion may not be initiated until the corrosion potential reaches the breakdown potential. Models for cathode modification support this hypothesis. More data may be necessary to generalize this hypothesis by reducing associated uncertainties.
4. Before the complete repassivation of crevice corrosion after initiation, the pit density inside the crevice is decreased. During the crevice corrosion propagation in the severe environments, the deepest penetration of corrosion is confined to a small area.
5. Models for the induction for localized corrosion were evaluated to assess whether laboratory tests could represent the very long-term performance in crevice corrosion. It

appears that data on the initiation time for crevice corrosion measured in the laboratory time scale may be suitable to represent performance for a very long period of time, given the appropriate environmental conditions.

5. References

- ASM International, ASM Handbook, Formally Ninth Edition, Metals Handbook, Volume 13. Corrosion, 1987
- P. Combrade, The Crevice Corrosion of Metallic Materials, MC TC R 01-1190, FRAMATOME ANP, 2001, Chapter 11 in *Corrosion Mechanisms in Theory and Practice*, second edition, edited by Ph. Marcus, Marcel Dekker, Inc., NY, 2002, p. 349
- D. S. Dunn, O. Pensado, Y.-M. Pan, R. T. Pabalan, L. Yang, X. He and K. T. Chiang, Passive and Localized Corrosion of Alloy 22—Modeling and Experiments, CNWRA 2005-02, Rev. 1, Center for Nuclear Waste Regulatory Analyses, San Antonio, TX, 2005
- D. S. Dunn, G. A. Cragolino and N. Sridhar, Long-Term Prediction of Localized Corrosion of Alloy 825 in High-Level Nuclear Waste Repository Environments, *Corrosion*, Vol. 52, p. 115, 1996
- X. He and D. S. Dunn, Crevice Corrosion Propagation Behavior of Alloy 22 in Extreme Environments, CORROSION 2007 CONFERENCE & EXPO, Paper No. 07578, NACE International, Houston, TX, 2007
- X. He and D. S. Dunn, Crevice Corrosion Penetration of Alloy 22 in Chloride-Containing Waters—Progress Report, CNWRA 2006-001, Center for Nuclear Waste Regulatory Analyses, San Antonio, TX, 2005
- L. F. Lin, C. Y. Chao and D. D. Macdonald, A Point Defect Model for Anodic Passive Films, II. Chemical Breakdown and Pit Initiation, *J. Electrochemical Society*, Vol. 128, p. 1194, 1981
- D. D. Macdonald, The Point Defect Model for the Passive State, *J. Electrochemical Society*, Vol. 139, P. 3434, 1992.
- D. D. Macdonald, A. Sun, N. Priyantha, and P. Jayaweera, An Electrochemical Study of Alloy 22 in NaCl Brine at Elevated Temperature: II. Reaction Mechanism Analysis, *J. Electroanalytical Chemistry*, Vol. 572, P. 421, 2004.
- T. Okada, Halide Nuclei Theory of Pit Initiation in Passive Metals, *J. Electrochemical Society*, Vol. 131, p. 241, 1984
- R. T. Pabalan, Chemistry of Water Contacting Engineered Barriers, NWTRB Workshop on Localized Corrosion of Alloy 22 in Yucca Mountain Environments, Las Vegas, NV, September 25-26, 2006, NRC ADAMS ML062640348, 2006

O. Pensado, Corrosion Model to Support Total System Performance Assessments, NWTRB Workshop on Localized Corrosion of Alloy 22 in Yucca Mountain Environments, Las Vegas, NV, September 25-26, 2006, NRC ADAMS ML062640354, 2006

M. Rodriguez, M. Stuart and R. Rebak Long Term Electrochemical Behavior of Creviced and Non-Creviced Alloy 22 in $\text{CaCl}_2 + \text{Ca}(\text{NO}_3)_2$ Brines at 155 EC, CORROSION 2007 CONFERENCE & EXPO, Paper No. 07577, NACE International, Houston, TX, 2007

T. Shinohara, S. Fujimoto, N. J. Laycock, A. Msallem, H. Ezuber and R. C. Newman, Numerical and Experimental Simulation of Iron Dissolution in a Crevice with a Very Dilute Bulk Solution, J. Electrochemical Soc., Vol. 144, p. 3791, 1997

P. K. Shukla, R. Pabalan, T. Ahn, L. Yang, X. He and H. Jung, Cathodic Capacity of Alloy 22 in the Potential Yucca Mountain Repository Environment, CORROSION 2008, New Orleans, Louisiana, U.S. Nuclear Regulatory Commission ADAMS ML080630670, 2008

N. Sridhar, G. Cragolino and D. Dunn, Experimental Investigations of Failure Processes of High-Level Radioactive Waste Container Materials, CNWRA 95-010, Center for Nuclear Waste Regulatory Analyses, San Antonio, TX, 1995

Z. Szklarska-Smialowska, *Pitting Corrosion of Metals*, National Association of Corrosion Engineers, Houston, TX, 1986

M. Urquidi-Macdonald and D. D. Macdonald, Theoretical Distribution Functions for the Breakdown of Passive Films, J. Electrochemical Society, Vol. 134, P. 41, 1987

J. C. Walton, G. Cragolino and S. K. Kalandros, A Numerical Model of Crevice Corrosion for Passive and Active Metals, Corrosion Science, Vol. 38, P. 1, 1996

Disclaimer

The NRC staff views expressed herein are preliminary and do not constitute a final judgment or determination of the matters addressed. This paper was prepared to document work performed by the Center for Nuclear Waste Regulatory Analyses (CNWRA) for NRC under Contract No. NRC-02-07-006. The activities reported here were performed on behalf of the NRC Office of Nuclear Material Safety and Safeguards, Division of High-Level Waste Repository Safety. This report is an independent product of the CNWRA and does not necessarily reflect the view or regulatory position of the NRC.